**Atmospheric
Measurement
Techniques**

A new CF-IRMS system for quantifying stable isotopes of carbon monoxide from ice cores and small air samples

Z. Wang and J. E. Mak

Institute for Terrestrial and Planetary Atmospheres, School of Marine and Atmospheric Sciences, Stony Brook University, Stony Brook, NY, USA

Abstract. We present a new analysis technique for stable isotope ratios ($\delta^{13}C$ and $\delta^{18}O$) of atmospheric carbon monoxide (CO) from ice core samples. The technique is an online cryogenic vacuum extraction followed by continuous-flow isotope ratio mass spectrometry (CF-IRMS); it can also be used with small air samples. The CO extraction system includes two multi-loop cryogenic cleanup traps, a chemical oxidant for oxidation to CO_2, a cryogenic collection trap, a cryofocusing unit, gas chromatography purification, and subsequent injection into a Finnigan Delta Plus IRMS. Analytical precision of 0.2‰ ($\pm 1\sigma$) for $\delta^{13}C$ and 0.6‰ ($\pm 1\sigma$) for $\delta^{18}O$ can be obtained for 100 mL (STP) air samples with CO mixing ratios ranging from 60 ppbv to 140 ppbv ($\sim$268–625 pmol CO). Six South Pole ice core samples from depths ranging from 133 m to 177 m were processed for CO isotope analysis after wet extraction. To our knowledge, this is the first measurement of stable isotopes of CO in ice core air.

1 Introduction

Atmospheric CO plays a key role in global atmospheric chemistry as the main sink for hydroxyl radicals (OH), therefore, strongly affecting the oxidizing capacity of the atmosphere (Crutzen and Zimmermann, 1991; Logan et al., 1981; Thompson, 1992). The major sources of CO in the modern atmosphere are known (Seiler, 1974). Different sources producing atmospheric CO with distinct ratios of $^{13}C/^{12}C$ and $^{18}O/^{16}O$ have been observed (Kato et al., 1999a, b; Stevens et al., 1972; Stevens and Wagner, 1989; Brenninkmeijer and Rockmann, 1997). Stable isotope ratios ($\delta^{13}C$ and $\delta^{18}O$) in atmospheric CO help to resolve the contributions of certain sources and, thus, to better estimate

the global CO budget (Mak and Kra, 1999; Rockmann et al., 2002; Manning et al., 1997). The CO budget calculated by three-dimensional inverse modelling is more robust with stable isotope (^{13}C and ^{18}O) data than with CO mixing ratios alone (Bergamaschi et al., 2000a; Bergamaschi et al., 2000b). But essentially no observations exist to provide information about relative source strengths during preindustrial times. The stable isotopes from air bubbles trapped in ice cores provide information on CO source strengths in the past. The typical volume of air trapped in ice cores is around 100 mL (STP) per kg of ice, and the CO mixing ratio in Antarctic ice cores is only $\sim$50 ppbv (Haan et al., 1996; Haan and Raynaud, 1998). The amount of CO trapped in 1 kg ice is only around 0.2 nmol. The sample size requirements for a conventional dual inlet method are mostly determined by the minimum operating pressure needed to generate a reasonable current at the collector end, which is in the order of 0.1 µmol (Merritt and Hayes, 1994). Therefore, the limited sample size of ice core air makes measuring CO isotope composition challenging.

Continuous-flow isotope ratio mass spectrometry (CF-IRMS) systems allow the analysis of small volumes. They have been developed to measure atmospheric CH_4 (Rice et al., 2001; Merritt et al., 1995; Lowe et al., 1991), atmospheric N_2O (Rockmann et al., 2003), atmospheric H_2 (Rhee et al., 2004) and volatile organic compounds (VOC) in ambient air (Rudolph et al., 1997). CF-IRMS was first demonstrated by Mak and Yang (1998) for CO isotope analysis by monitoring the relative abundances of masses 44, 45, and 46 of CO derived CO_2. A recent study by Tsunogai et al. (2002) has shown the advantage of isotope analysis for atmospheric CO using CF-IRMS by simultaneously monitoring the CO^+ ion currents at masses 28, 29, and 30. However, preparing CO standard gas with known isotope ratios and purifying CO presents different challenges. Because high precision mass spectrometry is usually based on CO_2 (Brenninkmeijer, 1999), in the present study we use the technique
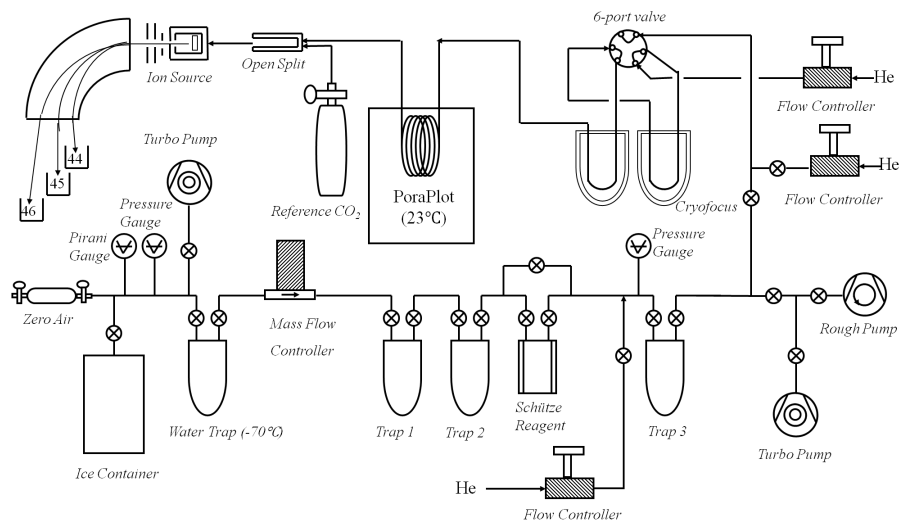
Fig. 1. A schematic diagram of the system used for mixing ratio, δ^{13}C and δ^{18}O analysis of atmospheric CO and ice core CO. See details in the text.

of oxidizing CO to CO_2 (Brenninkmeijer, 1993; Stevens and Krout, 1972). Here we present a new cryogenic vacuum extraction system designed to analyse isotope ratios of CO for small air samples ($\sim$268–625 pmol CO). We use this new system to measure isotope ratios of CO in air bubbles trapped in Antarctic ice cores.

2 Methodology

2.1 Instrumentation and procedure

A schematic diagram of the online extraction and preconcentration method for carbon and oxygen isotope analysis of ice core CO is shown in Fig. 1. A wet extraction system for ice cores is combined with a cryogenic vacuum system for CO extraction. The cryogenic vacuum extraction system and a stripped down commercially available Finnigan Preconcentration unit is attached to a Finnigan Delta Plus IRMS through a customized open split. The cryogenic vacuum extraction system includes dual four-loop glass coil (1/8 inch ID) cryogenic cleanup traps held at liquid nitrogen temperature, a Schütze reactor (1/8 inch ID U tube, 15 cm long) and a four loop-glass CO_2 collection trap held at liquid nitrogen temperature.

Ambient air samples are attached to the inlet of the cryogenic vacuum extraction system. The air passes through the cryogenic cleanup traps with a flow rate of 50 mL/min and atmospheric CO_2, H_2O, N_2O and other condensable species are removed due to condensation at liquid nitrogen temperature (Brenninkmeijer, 1993). The purified CO is then selectively and quantitatively oxidized to CO_2 by the Schütze reagent, retaining the original oxygen atom of CO (Brenninkmeijer, 1993). The Schütze reagent is prepared using a

slightly modified procedure than described in previous studies, in which the I_2O_5/H_2SO_4 on silica gel is flushed with ultrapure dry air flow instead of pumping during the baking process (Schütze, 1949; Smiley, 1965). A bypass is installed for the Schütze reactor tube so that the efficiency of CO_2 removal can be evaluated. The bypass also allows continuous back-flushing of the system with ultrapure helium between sample conversions.

The CO-derived CO_2 collected in trap 3 is eluted with cryogenically purified ultrapure helium at a flow rate of 40 mL/min for 5 min, then cryogenically focused in a microvolume trap of the modified Finnigan preconcentration unit through a Valco six-port valve (Fig. 1). The cryofocus trap is then heated to room temperature and the CO_2 is loaded on the gas chromatographic column (Chrompack PoraPLOT Q, 25 m$\times$0.25 mm) at a helium flow of 1 mL/min provided by the back inlet of the gas chromatographer. The derived CO_2 then passes through an open split into the Finnigan Delta Plus isotope ratio mass spectrometer (IRMS) at a flow rate of about 0.4 mL/min. The mass spectrometer reference CO_2 (Fig. 1) is a certified reference calibrated relative to the internationally accepted IAEA primary standard (δ^{13}C of -40.73‰ PDB and a δ^{18}O of 10.39‰ VSMOW, Oztech Trading Corporation, Safford, AZ).

The detailed calculation of δ^{13}C and δ^{18}O is based on the two observable ion-current ratios (45/44 and 46/44; Santrock et al., 1985) δ^{13}C of the original CO is determined by the δ^{13}C of derived CO_2, whereas δ^{18}O is based on a calibration gas (Brenninkmeijer, 1993). The mixing ratio of CO for an air sample is determined by the ratio of peak areas between the sample and a calibration gas.

The online wet extraction line for South Pole ice core samples is also shown in Fig. 1. The ice container is a 1.2 L borosilicate glass cylindrical container (100 mm ID) with a glass flange (100 mm ID), Viton o-ring (size 348) and external horseshoe clamp. The original part is from Chemglass Life Sciences (Vineland, NJ) and is modified by Universal Instrument Company, Palatine, IL. A four-loop coil trap (1/8 inch ID) with a volume of 15 mL is made of borosilicate glass and has both sides equipped with hi-vacuum stopcocks and Viton o-rings. The trap held at −70°C lies between the ice container and the inlet of the cryogenic vacuum system and is used to remove water vapour. Upon melting, the air sample released from ice core samples is then processed and analysed with the CF-IRMS method.

3 Diagnostic experiments

Diagnostic experiments conducted on the cryogenic extraction system include system blank tests, reproducibility tests, and accuracy tests. The system blank refers to the background signal from the entire analysis system including the background signal from Schütze reagent (Schütze blank) and from ice preparation and extraction (ice blank). The air sample signal is corrected by subtraction of the Schütze blank, therefore, the measurement of the Schütze blank is crucial for the correction of sample signals. While the origin of the Schütze blank is not clear, it is likely that impurities from the ingredients used to make the reagent are responsible for the majority of the blank signal. Another possibility is outgassing from the Viton o-rings, however, after three years of use the blank signal has not changed more than 10%. All Viton o-rings were originally baked out at 130 °C for 24 h after which the blank was unchanged. For ice core measurement, besides Schütze blank, there is another source of blank from ice preparation and extraction, which is called ice blank in this study. The sum of these two blanks is system blank for ice core measurement and will be applied to ice core sample correction, thus, the measurement of the system blank is crucial for the correction of ice core sample signals.

To quantify the Schütze blank signal, a flow of zero air devoid of any CO was processed through the reagent. Zero air was generated by passing ambient air through a platinum catalyst heated to 200 °C followed by a molecular sieve trap to remove the remaining CO_2, H_2O, N_2O and non-methane hydrocarbons (Mak, 1992). The ice blank is determined using artificial bubble-free ice from Laboratoire de Glaciologie et Géophysique de l'Environnement (LGGE), Grenoble, France. A calibration gas is loaded into the ice container after ice is evacuated and mimics the air released from ice core samples. The other procedure to process bubble-free ice is the same as analysing ice core samples which will be discussed in the ice core introduction section. The accuracy and reproducibility of data on stable carbon and oxygen isotopes

were determined using a calibration gas with a known isotope ratio as well as field air samples which will be described below.

4 Calibration gas test

Experiments were periodically performed to determine the accuracy and reproducibility of stable C and O isotope data using a calibration gas. The calibration gas, which is called secondary calibration gas in the present study, was CO mixed with ultrapure air, stored in an electropolished aluminum cylinder (Scott-Marrin, Inc, Riverside, CA) with an initial pressure of 1500 psi. The secondary calibration gas was first analysed using a conventional offline extraction (Mak et al., 1994) followed by dual inlet microvolume analysis with Finnigan Delta Plus IRMS (Brenninkmeijer, 1993; Mak and Brenninkmeijer, 1994). CO concentration was measured volumetrically by the conventional offline method (Mak and Brenninkmeijer, 1994) and $\delta^{13}C$ was measured with the dual inlet method (Brenninkmeijer, 1993; Mak and Brenninkmeijer, 1994).

A primary calibration gas (Scott-Marrin) is routinely processed using the offline method (Mak and Brenninkmeijer, 1994) to evaluate the performance of the offline extraction method and provides $\delta^{18}O$ of its Schütze reagent. The primary calibration gas has $\delta^{13}C$ of −39.8±0.1‰ VPDB (Mak and Brenninkmeijer, 1994) and $\delta^{18}O$ of 11.36±0.3‰ VS-MOW (C. Brenninkmeijer, personal communication, 2010; Brenninkmeijer, 1993). $\delta^{18}O$ of CO in the secondary calibration gas was retrieved based on the primary calibration gas measurements (Mak and Kra, 1999; Mak et al., 2003) according to the following equation:

$$\delta^{18}O(permil, VSMOW)_{2nd\ CalCO} = 2\delta^{18}O_{2nd\ CalCO_2}$$
$$-\left(2\delta^{18}O_{1st\ CalCO_2} - \delta^{18}O_{1st\ Cal\ CO}\right) \quad (1)$$

where $\delta^{18}O(permil, VSMOW)_{2nd\ CalCO}$ is the $\delta^{18}O$ of CO in the secondary calibration gas, $\delta^{18}O_{2nd\ CalCO_2}$ is the measured $\delta^{18}O$ of CO_2 derived from the secondary calibration gas, $\delta^{18}O_{1st\ Cal\ CO_2}$ is the measured $\delta^{18}O$ of CO_2 derived from the primary calibration gas, and $\delta^{18}O_{1st\ Cal\ CO}$ is the $\delta^{18}O$ of CO in the primary calibration gas (11.36‰ VSMOW). The $\delta^{18}O$ of the secondary calibration gas was, thus, determined by the same procedure as that of a sample, with the exception that the primary calibration was used as a reference, whereas samples were analysed relative to the secondary calibration gas.

The secondary calibration gas was then routinely processed in the new cryogenic extraction system with a flow rate of 50 mL/min and a collection time of 2 min and the following CF-IRMS to evaluate the performance of the new system. The peak area of the secondary calibration gas signal is used to calculate the CO concentration in field air samples and ice core samples. Since $\delta^{13}C$ were measured directly

using the offline method (Brenninkmeijer, 1993; Mak and Brenninkmeijer, 1994) and the new online method independently, $\delta^{13}C$ measurement between these two methods was used to evaluate the accuracy of the new online method in this study. $\delta^{18}O$ of the derived CO_2 from the secondary calibration gas was used for determining the $\delta^{18}O$ of the Schütze reagent and retrieving the original $\delta^{18}O$ of CO for samples based on the following equation:

$$\delta^{18}O(permil, VSMOW)_{sample} = 2\delta^{18}O_{CO_2}$$
$$-\left(2\delta^{18}O_{2nd\,Cal\,CO_2} - \delta^{18}O_{2ndCal\,CO}\right) \tag{2}$$

where $\delta^{18}O(permil, VSMOW)_{sample}$ is the original $\delta^{18}O$ of CO in samples, $\delta^{18}O_{CO_2}$ is the measured $\delta^{18}O$ of CO_2 derived from sample CO, $\delta^{18}O_{Cal\,CO_2}$ is the measured $\delta^{18}O$ of CO_2 derived from the CO in the secondary calibration gas, and $\delta^{18}O_{Cal\,CO}$ is the $\delta^{18}O$ of CO in the secondary calibration gas, which is determined by Eq. (1). The reproducibility of $\delta^{13}C$ and $\delta^{18}O$ of the replicates of secondary calibration gas analysed using the new online method was used to evaluate the precision of the method.

5   Field sample measurement

Air samples with the whole volume in the order of 600 l (STP) were collected into high-pressure aluminum air cylinders from the Mauna Loa Observatory and Westmann Islands, Iceland using a previously published protocol (Mak and Brenninkmeijer, 1998). These field samples were first processed with offline extraction and analysed with the conventional dual inlet-microvolume method, by which several hundred litres of the samples were processed. Aliquots of the samples were then processed with the new cryogenic extraction line with 50 mL/min flow rate and 2 min collection time and analysed by the following CF-IRMS. 4 to 12 replicates were measured for each sample to give the analytical reproducibility of CO concentration, $\delta^{13}C$, and $\delta^{18}O$ using this new method. CO concentration was calculated using the following equation:

$$C_S = C_C \cdot V_C/V_S \cdot (PA_S - PA_B)/(PA_C - PA_B) \tag{3}$$

where C_S is the CO concentration of a field sample, C_C is the CO concentration of the secondary calibration gas, V_C is the volume of the secondary calibration gas, V_S is the volume of a field sample, PA_S is the raw peak area of a field air sample CO, PA_B is the peak area of the Schütze blank, and PA_C is the raw peak area of the calibration gas according to a volume of V_C. A mass balance calculation based on the peak area and isotope ratios of both the Schütze blank peak and sample peak was applied to subtract the blank signal from the sample signal. The isotope ratios of a field air sample were calculated using the following equation:

$$\delta = (\delta_S \cdot PA_S - \delta_B \cdot PA_B)/(PA_S - PA_B) \tag{4}$$

where δ is the $\delta^{13}C$ or $\delta^{18}O$ of a field sample, δ_S is the $\delta^{13}C$ or $\delta^{18}O$ of the measurement value, δ_B is the $\delta^{13}C$ or $\delta^{18}O$ of the Schütze blank, PA_S is the peak area of a field air sample, PA_B is the peak area of the Schütze blank. Here the flow rate and collection time of the runs for field sample, calibration gas, and Schütze blank is 50 mL/min and 2 min.

The measurements of CO concentration, $\delta^{13}C$, and $\delta^{18}O$ with the new online continuous flow method were compared with those using the offline extraction and dual inlet method (Brenninkmeijer, 1993; Mak and Brenninkmeijer, 1994). The primary calibration gas was analysed using the conventional dual inlet method to evaluate the accuracy and showed no bias (Mak and Brenninkmeijer, 1994). The field samples were measured by these two methods independently. CO concentration measurement using the offline method was determined by manometry of the CO-derived CO_2 and the volume of displaced air, whereas that using the new online method was determined by ratio of peak area (Eq. 3). $\delta^{13}C$ measurement using the offline method was determined by dual inlet analysis, whereas that using the new online method was determined by CF-IRMS and Eq. (4). $\delta^{18}O$ measurement using the offline method was determined by dual inlet analysis and the primary calibration gas measurements, whereas that using the new online method was determined by CF-IRMS and the secondary calibration measurements. Therefore, the differences of the measurements between these two methods reflect the accuracy of the new online method.

6   Ice core introduction

South Pole ice core samples were provided by the US National Ice Core Laboratory (NICL), Boulder, Colorado. They were dry drilled by Jihong Cole-Dai and his colleagues in 2004 at South Pole (89°57′ S 17°36′ W). They contain negligible contamination since no kerosene fluid was used for drilling. The ice core samples were semi-cylindrical with an average length of 17 cm and radius of 5 cm and were prepared for analysis in a cold room held at −20 °C. The ice core samples were first trimmed with a band saw to remove around 5 mm of surface and then scraped with a stainless steel disposable scalpel to remove an additional 1–2 mm of surface. The ice core sample was weighed and then sealed in a previously prepared container that had been thoroughly cleaned with acetone, rinsed three times with Milli-Q water and heated overnight at 90 °C. The sealed container was then immersed in a cooling bath held at −20 °C. A 1/4″ glass multiloop water trap between the container and the inlet of the cryogenic vacuum extraction system was held at −70 °C. The ice and container were evacuated and flushed with zero air three times for 10 min. Then the ice was melted by placing the container in a water bath held at a temperature of 60–70 °C. The melting takes around 25 min. After

melting, the air extracted from the ice was processed through the cryogenic vacuum extraction system and loaded into the CF-IRMS.

As the ~1 kg ice core sample melted, ~100 mL (STP) air sample was released, giving an initial pressure in the headspace of the ice container about 300 mbar. During ice core air extraction, the mass flow controller (MFC, Fig. 1) causes a flow restriction due to a lack in pressure difference across the MFC, resulting in a long ice processing time. However, for regular field air sample and routine calibration measurements, a MFC is required to control the flow and to quantify the volume of air processed. The headspace pressure drops to 60 mbar after the air sample was processed for 5 min, at which time a 150 mL glass flask filled with zero air was expanded into the ice container to build up pressure to around 500 mbar. The mixed air was processed for another 5 min. The total processing time is 10 min. The ratio of final pressure to the initial pressure of each step shows how much sample remains in the container. The total percentage of the original air processed for the two steps is calculated according to the following equation:

$$P = 1 - P2/P1 \cdot P4/P3 \qquad (5)$$

where P is the total percentage of the original air processed, P1 is the initial headspace pressure after air released from ice, P2 is the pressure after 5 min processing, P3 is the pressure after loading zero air, and P4 is the final pressure after 10 min processing. Temperature of water in the ice container is close to 0° after ice melts. The pressure measurements were corrected for saturated water vapour pressure at this temperature (6.1 mbar) (Murphy and Koop, 2005). The percentage of the original air processed is calculated to be around 95%. The flow rate signal of the MFC during the extraction is monitored by a data acquisition device (Labjack Corporation, Lakewood, CO) and Labview program. The volume of air processed for each step is, thus, integrated by the real time flow rate data. The total volume of the released air sample processed is determined by the pressure and the integrated volume based on real time flow rate based on the following equation:

$$V_S = V1 + V2 \cdot P2/P3 \qquad (6)$$

where V_S is the total volume of air processed for the ice core sample, V1 is the integrated volume for 5 min extraction, V2 is integrated volume for the second 5 min extraction, and P2 and P3 are the same as above. CO concentration of ice core samples is then calculated according to Eqs. (6) and (3), with system blank subtracted from sample signal. Based on this volume calculation, the water vapour pressure (6.1 mbar) only causes a 2% difference. Isotope ratios were calculated according to Eq. (4). Uncertainties for ice core measurements include both the analysis reproducibility and the error propagation of calculations.

7 Results and discussion

7.1 System blank

The Schütze blank was measured to be lower than 40 pmol CO (9 ppbv at STP) for a 100 mL air sample with a flow rate of 50 mL/min and a collection time of 2 min. The relationship between Schütze blank and collection time was studied. The Schütze blank signal was observed to be dependent on the collection time and was measured to be 72±3 pmol CO (16.1±0.7 ppbv at STP for a 100 mL air sample) for a collection time of 10 min and a flow rate of 50 mL/min (Table 1). A linear relationship was found between Schütze blank signal and collection time: C=3.84·t+30.8, where C is the Schütze blank signal and t is the collection time. Schütze blank increases with collection time, indicating one unknown contribution to the background is time dependent. The intercept shows a large portion of the blank is time independent, which might be from the Schütze and has not decreased significantly for two years. The relationship between Schütze blank and flow rate has also been studied and measurements are shown in Table 2. With a collection time of 2 min or 10 min, the Schütze blank signal showed independence of flow rate between 10 mL/min and 100 mL/min.

The δ^{13}C and δ^{18}O for all the Schütze blank results (Tables 1 and 2) is −15.2±0.3‰ and 33.6±0.4‰, respectively. The isotope ratios of the Schütze blank were independent on collection time, sample size and flow rate. The Schütze blank signal was also found to be independent of the amount of zero air since the CO in zero air was estimated to be smaller than 1 ppbv based on an offline extraction method (Mak and Brenninkmeijer, 1994).

The ice core analysis system blank includes the total amount of Schütze blank and ice blank. The former was determined to be 72±2 pmol for a collection time of 10 min (Table 2). The system blank was determined using artificial bubble-free ice and the secondary calibration gas. The system blank CO concentration was taken as difference between the measured CO concentration for calibration with bubble-free ice and the CO concentration of secondary calibration gas. The system blank CO concentration was calculated with the following equation:

$$C_B = C_C \cdot V_C/V_I \cdot PA_I/PA'_C - C_C \qquad (7)$$

where C_B is the system blank CO concentration, C_C is the CO concentration of the secondary calibration gas, V_C is the volume of secondary calibration gas, V_I is the volume of air processed in the bubble-free ice tests and determined by Eq. (6), PA_I is the peak area of calibration in ice condition, PA'_C is the peak area of secondary calibration gas according to a volume of V_C and equals to $PA_C - PA_B$ in Eq. (3). The isotope ratios of system blank were calculated using the following equations:

$$\delta = (\delta_I \cdot PA_I - \delta_C \cdot PA''_C)/(PA_I - PA''_C) \qquad (8)$$

Table 1. Schütze blank of the cryogenic system using zero air at a different collection time and with a flow rate of 50 mL/min.

Sample Volume (mL)	Collection time (min)	CO blank (pmol)	$\delta^{13}C$ (‰, VPDB)	$\delta^{18}O$ (‰, VSMOW)
100	2	37±3	−15.2±0.3	33.4±0.3
250	5	49	−15.6	33.0
500	10	72±3	−15.3±0.3	33.9±0.4
750	15	89	−15.3	33.9
1500	30	145	−15.0	33.8

Table 2. Schütze blank of the cryogenic system using zero air at a different flow rate.

Sample Volume (mL)	Flow rate (mL/min)	Collection time (min)	CO blank (pmol)	$\delta^{13}C$ (‰, VPDB)	$\delta^{18}O$ (‰, VSMOW)
20	10	2	39±1	−15.8±0.3	34.1±0.4
50	25	2	36±0.3	−15±0.4	33.9±0.2
100	50	2	37±3	−15.2±0.3	33.4±0.3
150	75	2	40±2	−15.6±0.4	33.2±0.5
200	100	2	40±2	−15.3±0.3	33.2±0.5
100	10	10	72	−15.1	33.3
250	25	10	72±5	−15.7±0.2	33.6±0.4
500	50	10	72±3	−15.3±0.3	33.9±0.4
750	75	10	69	−15.1	34.1
1000	100	10	74	−15.5	33.8

$$PA''_C = PA'_C \cdot V_I / V_C \qquad (9)$$

where δ is the $\delta^{13}C$ or $\delta^{18}O$ of system blank, δ_I is the $\delta^{13}C$ or $\delta^{18}O$ of the measurement value, δ_C is the $\delta^{13}C$ or $\delta^{18}O$ of secondary calibration gas, PA_I, PA'_C, V_I, and V_C are the same as those in Eq. (7), PA''_C is the expected peak area of calibration gas in ice condition according to a volume of V_I.

The long processing time and the concomitant large blank from the Schütze reagent limit the precision of isotope ratios measured using this technique. To shorten the processing time and decrease the Schütze blank, we attempted to use adsorbents such as molecular sieve 5A and molecular sieve 13X held at liquid nitrogen temperature to condense the air released from ice cores. However, the molecular sieves caused isotope fractionation of both carbon (2–3‰) and oxygen (4‰), thus, these adsorbents were no longer applied. The use of a Teflon beaker liner (Welch Fluorocarbon Inc.) was also tried, as its volume was adjustable and, thus, could contribute to a buildup of pressure in the headspace by shrinking and pushing water upward. However, the permeability of Teflon for major components of air limited the use of this material. Tedlar (polyvinyl fluoride), another polyfluorocarbon was investigated as a low-permeability substitute for Teflon. The rigidity of Tedlar film made engineering a Tedlar liner quite difficult and gives no real advantage. In the end, while the idea of reducing the size of the Schütze blank is intriguing and may warrant further study, we opted to keep our sampling protocol simple and characterised the Schütze

blank to a high degree of precision. For future study, an old fashioned mercury toepler pump could be ideal for solving this problem by reducing extraction time and Schütze blank (Brenninkmeijer, 1983).

An initial high system blank of 200 pmol CO was thought to be caused by CO adsorption on the ice surface. The blank decreased significantly to a level of 90 pmol CO after ice and container were evacuated and flushed with zero air three times. Further flushing with zero air did not reduce the system blank further. The bubble-free ice was also tested under light and dark environments to rule out the possibility of photochemical production. The isotope composition ($\delta^{13}C=−15‰$) of the system blank and the similar blank signal between light and dark environment indicates that the ice blank is from air diffusion/adsorption – not in situ photochemical production – since $\delta^{13}C$ of CO from oxidation processes is much lower (Stevens and Wagner, 1989). The six measurements of system blank are shown in Table 3. The measured system blank is 90±8 pmol. The $\delta^{13}C$ and $\delta^{18}O$ of system blank is −15.3±0.3‰ and 33.4±0.5‰, respectively. The uncertainties in CO concentration and isotope ratios in system blanks, which will be used for evaluating the uncertainties of ice core samples, are ascribed to random error in preparing bubble-free ice samples. The system blank signal is subtracted from the sample signal by a mass balance calculation. The system blank is crucial for the ice core data since it accounts for ~30% of the total signal and the CO blank

Table 3. System blank using calibration gas and artificial bubble-free ice.

Artificial ice sample #	Artificial ice type	Weight (g)	CO blank[a] (pmol)	$\delta^{13}C$ (‰, VPDB)	$\delta^{18}O$ (‰, VSMOW)
1	Polycrystalline ice	256	90	−15.4	34.0
2	Polycrystalline ice	385	99	−15.3	32.9
3	Monocrystalline ice	200	77	−15.6	33.6
4	Monocrystalline ice[b]	275	90	−15.0	33.3
5	Monocrystalline ice	150	99	−14.9	32.9
6	Monocrystalline ice	347	86	−15.3	33.7

Note: [a]: system blank including Schütze blank and ice blank; [b]: Dark test: glass container was wrapped with aluminum foil during the experiment.

Table 4. Comparison of $\delta^{13}C$ and $\delta^{18}O$ results of field CO samples obtained by dual inlet microvolume analysis and online extraction CF-IRMS.

Sample ID	Collection Date	[CO] (ppbv)	SD[a]	$\delta^{13}C$ (‰, VPDB)	SD[a]	$\delta^{18}O$ (‰, VSMOW)	SD[a]	Sample Volume (L)	[CO] (ppbv)	SD	$\delta^{13}C$ (‰, VPDB)	SD	$\delta^{18}O$ (‰, VSMOW)	SD	Sample Volume (L)
				Dual inlet microvolume analysis							On-line extraction CF-IRMS				
315MLCO (12)[b]	28-Aug-07	61	3	−31.00	0.4	−1.27	0.5	286	62	1	−30.80	0.17	−1.33	0.61	0.1
393ICE(5)	24-Jan-07	126	3	−27.19	0.4	8.74	0.5	658	125	2	−27.45	0.28	8.49	0.20	0.1
394ICE(7)	31-Jan-07	128	3	−27.25	0.4	8.25	0.5	678	124	2	−27.36	0.24	8.35	0.38	0.1
396ICE(4)	17-Jan-07	137	3	−27.63	0.4	9.16	0.5	662	139	1	−27.84	0.19	9.39	0.36	0.1
397ICE(4)	07-Feb-07	134	3	−27.58	0.4	8.19	0.5	602	137	2	−27.71	0.10	8.32	0.21	0.1
398ICE(5)	28-Feb-07	139	3	−26.93	0.4	9.64	0.5	674	144	4	−27.15	0.28	9.43	0.38	0.1

Note [a]: this standard deviation (±1 σ) for dual inlet includes both analytical error for mass spectrometric analysis and sample preparation error (Mak and Brenninkmeijer, 1994).
[b]: the number in parentheses next to sample ID is the number of analyses by online extraction CF-IRMS.

applied for each sample. The evaluation of the blank correction to the uncertainty of ice core samples will be discussed later in this paper.

8 Calibration gas

The CO concentration of the secondary calibration gas was measured to be 141 ppbv based on the primary calibration on National Oceanic and Atmospheric Administration/Climate Monitoring and Diagnostics Laboratory (NOAA/CMDL) CO reference scale. $\delta^{13}C$ of CO in the secondary calibration gas was measured to be −45.56‰ VPDB with the dual inlet method by the IRMS. $\delta^{18}O$ of CO in the secondary calibration gas was measured to be 2.44‰ VSMOW according to Eq. (1). The results of $\delta^{13}C$ of CO and $\delta^{18}O$ of derived CO_2 from the secondary calibration gas runs are shown in Fig. 2. The mean value of $\delta^{13}C$ is −45.40‰ (VPDB) with a standard deviation of 0.33‰ (±1σ) for 47 runs with CO amount ranging from 232 pmol to 4 nmol. The mean value of $\delta^{18}O$ of derived CO_2 from the secondary calibration gas is 0.42‰ (VSMOW) with a standard deviation of 0.32‰ (±1σ). $\delta^{13}C$ shows an offset of +0.16‰, which is smaller than the standard deviation of 0.33‰ (±1σ), indicating good performance of the line. This $\delta^{18}O$ value was used for determining the $\delta^{18}O$ of CO for air samples according to Eq. (2).

9 Field sample measurement

Measurements of 6 field air samples using the new online extraction CF-IRMS as well as the offline method are shown in Table 4. With a sample volume of only 0.1% of that used in the offline method, our new online analysis system still provided comparable precisions for both CO concentration and isotope ratios as the offline method. For this offline method, ±1σ standard deviation of CO concentration is 3 ppbv with sample preparation errors and for $\delta^{13}C$ and $\delta^{18}O$ is 0.4‰ and 0.5‰, respectively (Mak and Brenninkmeijer, 1994). Analytical precision of 2 ppb (±1σ) for CO mixing ratio, 0.2‰ (±1σ) for $\delta^{13}C$ and 0.6‰ (±1σ) for $\delta^{18}O$ were obtained for a sample size of 268 pmol CO (100 mL air sample with CO mixing ratio of 60 ppbv) from the new online analysis method. Notice that the sample from Mauna Loa can be used to assess the linearity of the system since its isotope ratios are very different from the others (Table 4). Considering the uncertainties, no significant difference for CO concentration, $\delta^{13}C$, and $\delta^{18}O$ was found between the offline dual inlet microvolume analysis and the online extraction CF-IRMS analysis, implying the reliable accuracy of the new online method.

Table 5. Online extraction CF-IRMS measurements for South Pole ice core CO.

Sample Depth (m)	Mean gas age (Yr AD)[c]	[CO] (ppbv)	SD (ppbv)	$\delta^{13}C$ (‰, VPDB)	SD (‰)	$\delta^{13}C$[d] (‰, VPDB)	$\delta^{18}O$ (‰, VSMOW)	SD (‰)	$\delta^{18}O$[d] (‰, VSMOW)	[CO]_blank (ppbv)	Ice weight (g)
135	1821±110	57	4	−28.83	0.4	−29.43	−1.79	1.1	−2.99	22	872
147	1688±110	39	4	−29.40	0.4	−30.00	−1.89	1.1	−3.09	18	877
157	1578±110	37	4	−29.15	0.4	−29.75	−1.02	1.1	−2.22	18	918
165T[a]	1490±110	42	4	−28.47	0.4	−29.07	−0.49	1.1	−1.69	18	922
165B[b]	1490±110	46	4	−28.95	0.4	−29.55	−0.96	1.1	−2.16	18	957
177	1358±110	57	4	−27.40	0.4	−28.00	1.43	1.1	0.23	22	939

Note [a]: 165 m top; [b] 165 m bottom. Standard deviation is based on the results from calibration runs with bubble-free ice processed the same way as that for real ice core samples. [c]: gas ages are linearly interpolated based on the gas age-depth relationship of South Pole ice core according to (Neftel et al., 1985; Schwander and Stauffer, 1984; Friedli et al., 1984); age errors are calculated according to (Friedli et al., 1984; Neftel et al., 1985; Schwander and Stauffer, 1984). [d]: Isotope ratios corrected by gravitational fractionation (Battle et al., 1996; Landais et al., 2006).
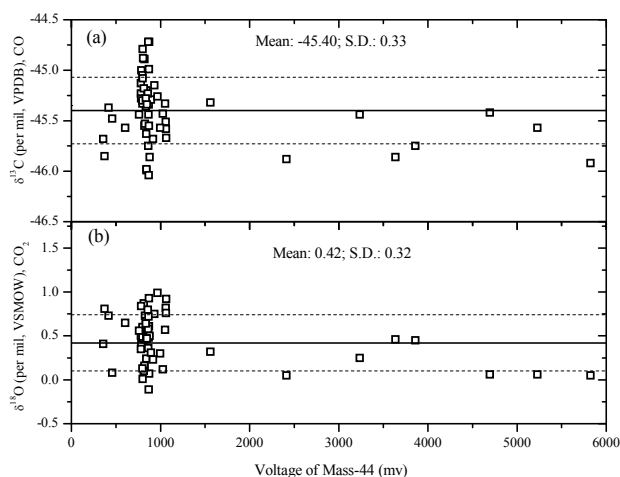

Fig. 2. Measurements of **(a)** $\delta^{13}C$ and **(b)** $\delta^{18}O$ for calibration gas versus voltage mass-44 ranging from 400 mv to 6 V. Mean value of $\delta^{13}C(CO)$: −45.40‰ (with standard deviation 0.33‰); mean value of $\delta^{18}O(CO_2)$: 0.42‰ (with standard deviation 0.32‰). Sample size is linear with voltage of mass-44 and 700 pmol CO gives 1 V for the signal of voltage mass-44.

10   South Pole ice core measurement

Six ice core samples were measured in this study. Results of the measurements of the 6 South Pole ice core samples, including both CO mixing ratios and isotope ratios, are shown in Table 5. CO concentration was calculated according to Eqs. (3) and (6), and the isotope ratios were calculated using the above Eq. (4). The system blank specified for each ice core sample (column 11 in Table 5) was the average of system blank before and after the ice core sample. Ice core sample at depths of 135 m and 177 m were measured after #2 artificial ice measurement and before #5 artificial ice measurement (Table 3), so the average of #2 and #5 system blank was specified for these two ice core samples. The other four ice core samples were measured after #3 artificial ice

measurement and before #6 artificial ice measurement (Table 3), so the average of #3 and #6 system blank was specified for the other four ice core samples.

The uncertainties are shown as standard deviations (SD, ±1σ) (Table 5) and calculated according to the error propagation of calculation and the reproducibility of bubble-free ice tests. The contribution of the system blank is as high as 30% and introduced uncertainties to ice core measurements due to the blank correction. The 3 ppbv uncertainty of CO concentration for field sample measurement and 9 pmol uncertainty of system blank determined the uncertainty of CO concentration of ice core samples to be 4 ppbv. According to the uncertainties of CO concentration (9 pmol) of system blank and Eq. (3), the correction of the blank introduced an uncertainty of 0.4‰ for $\delta^{13}C$ and 1.1‰ for $\delta^{18}O$. According to uncertainties of isotope ratios (0.3 for $\delta^{13}C$ and 0.5‰ for $\delta^{18}O$) of system blank, the correction introduced an uncertainty of 0.1‰ for $\delta^{13}C$ and 0.2‰ for $\delta^{18}O$. As a result, the uncertainty was calculated to be 0.4‰ for $\delta^{13}C$ and 1.1‰ for $\delta^{18}O$ for ice core samples. The signal/noise ratios for concentration and isotope ratios were larger than 3, indicating significant change in both CO concentration and isotope ratios.

The raw data for CO mixing ratio and isotope ratios shown have been corrected for gravitational fractionation according to the $\delta^{15}N$ measurement performed on South Pole firn (Battle et al., 1996; Landais et al., 2006). The gravitational effect for CO can be neglected (Haan and Raynaud, 1998). The isotope ratio corrections for $\delta^{13}C$ and $\delta^{18}O$ are −0.6‰ and −1.2‰, respectively (Battle et al., 1996; Landais et al., 2006). The corrected isotope ratios are also shown in Table 5. The consistency of CO mixing ratio and isotope ratios between the duplicate South Pole ice core samples at 165 m (AD 1490) indicate that the new analytical technique produces consistent results for ice core samples with a CO amount as low as 223 pmol.

Present-day observations at Scott Base (77.8° S, 167.5° E) indicate annual mean CO concentration is 51 ppbv with δ^{13}C and δ^{18}O is $-29.4‰$ VPDB and $-3.8‰$ VSMOW, respectively for the period 1993–1995 (Brenninkmeijer, 1993; Moss et al., 1998). Thus, CO concentrations at 135 m (AD 1821) and 177 m (AD 1358) are comparable with those in modern atmosphere, whereas CO concentration at 157 m (AD 1578) is around 20 ppbv lower than that in modern atmosphere. Furthermore, both δ^{13}C and δ^{18}O of the sample at 177 m (AD 1358) have a shift of isotope ratio larger than the gravitational fractionation compared with present-day values (Wang, 2009), showing real variations of CO isotope ratios in the past atmosphere.

Based on isotope mass balance calculation (Wang, 2009) and MOZART simulations on present CO source strengths (K. Park, personal communication, 2010), the 600 ppb of [CH$_4$] in 1500 will cause an enrichment of 2.6‰ for δ^{18}O in CO and 17 ppbv lower CO concentration compared with present day. A change of +50% biomass burning emission compared with present day's level causes an enrichment of 1.5‰ for δ^{18}O in CO and a change of -50% biomass burning emission causes a depletion of 1.9‰ for δ^{18}O in CO. A change of +50% NMHC oxidation compared with modern day level causes a depletion of 0.8‰ for δ^{18}O in CO and a change of -50% NMHC oxidation causes an enrichment of 1.0‰ for δ^{18}O in CO. Thus, the 4‰ change of δ^{18}O in CO in our ice core samples allows us to deduce useful information for the CO source strength in the preindustrial times.

The 20 ppbv variation of CO concentration indicates the change of the absolute source strength of CO in the past several centuries, while the ~1.4‰ variation of δ^{13}C and ~4‰ of δ^{18}O indicates the change of the relative source strength of CO such as biomass burning emission in the past atmosphere. This combined information allows us to reveal the biogeochemical causes of the variations of atmospheric CO budget such as variation of biomass burning emission due to the change of aridity/moisture and/or warmer/cooler temperature and the variation of biogenic emission of non-methane hydrocarbon from vegetation due to the change of temperature and vegetation area in the preindustrial times. The drop of CO concentration and depletion of both ^{13}C and ^{18}O in the 17th and 18th century suggests a drop of biomass burning in this period. CO from biomass burning in high latitude SH originates from the tropics (Edwards et al., 2006). It has been reported that biomass burning is more favourable with warmer ambient temperatures and dryer conditions (Carcaillet et al., 2002; Crutzen and Andreae, 1990). The suggested drop of biomass burning in this study is consistent with the cooler temperature and moist atmosphere in the tropics during the 17th and 18th century (Thompson et al., 2003; Verschuren et al., 2000), and it is also consistent with the biomass burning reconstruction from sedimentary charcoal record (Marlon et al., 2008).

11 Conclusions

Six South Pole ice core samples were analysed with a new technique using online cryogenic extraction and CF-IRMS analysis for simultaneous measurement of stable isotope ratios (δ^{13}C and δ^{18}O) of atmospheric CO in small air samples. The concentrations and isotope ratios provide important information on the source strengths of CO such as biomass burning emissions in preindustrial times and help to extrapolate the overall stability of tropospheric chemistry basics: CH$_4$-CO-OH cycle. Concentration, δ^{13}C, and δ^{18}O values for atmospheric CO with sample size as small as 220 pmol can be determined using this new technique with high precision. This new online technique is especially useful in characterising air samples with very small volume, such as atmospheric CO trapped in an ice core. This is to our knowledge the first measurement of CO isotopes in ice core samples.

References

Battle, M., Bender, M., Sowers, T., Tans, P. P., Butler, J. H., Elkins, J. W., Ellis, J. T., Conway, T., Zhang, N., Lang, P., and Clarke, A. D.: Atmospheric gas concentrations over the past century measured in air from firn at the South Pole, Nature, 383, 231–235, 1996.

Bergamaschi, P., Hein, R., Brenninkmeijer, C. A. M., and Crutzen, P. J.: Inverse modeling of the global CO cycle 2. Inversion of C-13/C-12 and O-18/O-16 isotope ratios, J. Geophys. Res.-Atmos., 105, 1929–1945, 2000a.

Bergamaschi, P., Hein, R., Heimann, M., and Crutzen, P. J.: Inverse modeling of the global CO cycle 1. Inversion of CO mixing ratios, J. Geophys. Res.-Atmos., 105, 1909–1927, 2000b.

Brenninkmeijer, C. A. M.: Deuterum, oxygen-18 and carbon-13 in tree rings and peat depositsin relation to climate, Ph.D. thesis, Univ. of Groningen, The Netherlands, 1983.

Brenninkmeijer, C. A. M.: Measurement of the abundance of [14]CO in the atmosphere and the ^{13}C/^{12}C and ^{18}O/^{16}O ratio of atmospheric CO with applications in New Zealand and Antarctica, J. Geophys. Res, 98, 10595–10614, 1993.

Brenninkmeijer, C. A. M. and Rockmann, T.: Principal factors determining the ^{18}O/^{16}O ratio of atmospheric CO as derived from observations in the southern hemispheric troposphere and lowermost stratosphere, J. Geophys. Res.-Atmos., 102, 25477–25485, 1997.

Brenninkmeijer, C. A. M.: Review of progress in isotope studies of atmospheric carbon monoxide, Chemosphere-Global Change Science, 1, 33–52, 1999.

Carcaillet, C., Almquist, H., Asnong, H., Bradshaw, R. H. W., Carrion, J. S., Gaillard, M. J., Gajewski, K., Haas, J. N., Haberle, S. G., Hadorn, P., Muller, S. D., Richard, P. J. H., Richoz, I., Rosch, M., Goni, M. F. S., von Stedingk, H., Stevenson, A. C., Talon, B., Tardy, C., Tinner, W., Tryterud, E., Wick, L., and Willis, K. J.: Holocene biomass burning and global dynamics of the carbon cycle, Chemosphere, 49, 845–863, 2002.

Crutzen, P. J. and Andreae, M. O.: Biomass burning in the tropics: impact on atmospheric chemistry and biogeochemical cycles, Science, 250, 1669–1678, 1990.

Crutzen, P. J. and Zimmermann, P. H.: The changing photochemistry of the troposphere, Tellus A, 43, 136–151, 1991.

Edwards, D. P., Emmons, L. K., Gille, J. C., Chu, A., Attie, J. L., Giglio, L., Wood, S. W., Haywood, J., Deeter, M. N., Massie, S. T., Ziskin, D. C., and Drummond, J. R.: Satellite-observed pollution from Southern Hemisphere biomass burning, J. Geophys. Res.-Atmos., 111, D14312, doi:10.1029/2005jd006655, 2006.

Friedli, H., Moor, E., Oeschger, H., Siegenthaler, U., and Stauffer, B.: [13]C/[12]C Ratios in CO_2 Extracted from Antarctic Ice, Geophys. Res. Lett., 11, 1145–1148, 1984.

Haan, D., Martinerie, P., and Raynaud, D.: Ice core data of atmospheric carbon monoxide over Antarctica and Greenland during the last 200 years, Geophys. Res. Lett., 23, 2235–2238, 1996.

Haan, D. and Raynaud, D.: Ice core record of CO variations during the last two millennia: atmospheric implications and chemical interactions within the Greenland ice, Tellus, 50B, 253–262, 1998.

Kato, S., Akimoto, H., Braunlich, M., Rockmann, T., and Brenninkmeijer, C. A. M.: Measurements of stable carbon and oxygen isotopic compositions of CO in automobile exhausts and ambient air from semi-urban Mainz, Germany, Geochem. J., 33, 73–77, 1999a.

Kato, S., Akimoto, H., Rockmann, T., Braunlich, M., and Brenninkmeijer, C. A. M.: Stable isotopic compositions of carbon monoxide from biomass burning experiments, Atmos. Environ., 33, 4357–4362, 1999b.

Landais, A., Barnola, J. M., Kawamura, K., Caillon, N., Delmotte, M., Van Ommen, T., Dreyfus, G., Jouzel, J., Masson-Delmotte, V., Minster, B., Freitag, J., Leuenberger, M., Schwander, J., Huber, C., Etheridge, D., and Morgan, V.: Firn-air δ15 N in modern polar sites and glacial-interglacial ice: a model-data mismatch during glacial periods in Antarctica?, Quaternary Sci. Rev., 25, 49–62, doi:10.1016/j.quascirev.2005.06.007, 2006.

Logan, J. A., Prather, M. J., Wofsy, S. C., and McElroy, M. B.: Tropospheric chemistry: a global perspective, J. Geophys. Res.-Oc. Atm., 86, 7210–7254, 1981.

Lowe, D. C., Brenninkmeijer, C. A. M., Tyler, S. C., and

Dlugkencky, E. J.: Determination of the Isotopic Composition of Atmospheric Methane and Its Application in the Antarctic, J. Geophys. Res.-Atmos., 96, 15455–15467, 1991.

Mak, J. and Kra, G.: The isotopic composition of carbon monoxide at Montauk Point, Long Island, Chemosphere: Global Change Science 1, 1, 205–218, 1999.

Mak, J., Kra, G., Sandomenico, T., and Bergamaschi, P.: The seasonally varying isotopic composition of the sources of carbon monoxide at Barbados, West Indies, J. Geophys. Res.-Atmos., 108, 4635, doi:10.1029/2003jd003419, 2003.

Mak, J. E.: The Isotopes of Carbon Monoxide in the Free Troposphere and Their Implications to Atmospheric Chemistry, PhD Thesis, The University of California, San Diego and National Center for Atmospheric Research, 1992.

Mak, J. E. and Brenninkmeijer, C. A. M.: Compressed-Air Sample Technology for Isotopic Analysis of Atmospheric Carbon-Monoxide, J. Atmos. Ocean Tech., 11, 425–431, 1994.

Mak, J. E., Brenninkmeijer, C. A. M., and Tamaresis, J.: Atmospheric [14]CO Observations and Their Use for Estimating Carbon Monoxide Removal Rates, J. Geophys. Res.-Atmos., 99, 22915–22922, 1994.

Mak, J. E. and Brenninkmeijer, C. A. M.: Measurement of [13]CO and C[18]O in the free troposphere, J. Geophys. Res., 103, 19,347–319,358, 1998.

Mak, J. E. and Yang, W.: Technique for Analysis of Air Samples for ^{13}C and [18]O in Carbon Monoxide via Continuous-Flow Isotope Ratio Mass Spectrometry, Anal. Chem., 70, 5159–5161, 1998.

Manning, M. R., Brenninkmeijer, C. A. M., and Allan, W.: Atmospheric carbon monoxide budget of the southern hemisphere: Implications of ^{13}C/^{12}C measurements, J. Geophys. Res.-Atmos., 102, 10673–10682, 1997.

Marlon, J. R., Bartlein, P. J., Carcaillet, C., Gavin, D. G., Harrison, S. P., Higuera, P. E., Joos, F., Power, M. J., and Prentice, I. C.: Climate and human influences on global biomass burning over the past two millennia, Nat. Geosci., 1, 697–702, doi:10.1038/ngeo313, 2008.

Merritt, D. A. and Hayes, J. M.: Factors controlling precision and accuracy in isotope ratio monitoring mass spectrometry, Anal. Chem., 66(14), 2336–2347, 1994.

Merritt, D. A., Hayes, J. M., and Marias, D. J. D.: Carbon Isotopic Analysis of Atmospheric Methane by Isotope-Ratio-Monitoring Gas-Chromatography Mass-Spectrometry, J. Geophys. Res.-Atmos., 100, 1317–1326, 1995.

Moss, R., Manning, M., Lowe, D., Ferretti, D., and Knobben, R.: Changes in atmospheric carbon monoxide in the pacific region, in: Preceedings of the Workshop on the Science of Atmospheric Trace Gases, edited by: Clarkson, T. S., 74–77, Natl. Inst. of Water and Atmos. Res., Wellington, New Zealand, 1998.

Murphy, D. M. and Koop, T.: Review of the vapour pressures of ice and supercooled water for atmospheric applications, Quart. J. Royal Met. Soc, 131, 1539–1565, 2005.

Neftel, A., Moor, E., Oeschger, H., and Stauffer, B.: Evidence from Polar Ice Cores for the Increase in Atmospheric CO_2 in the Past 2 Centuries, Nature, 315, 45–47, 1985.

Rhee, T. S., Mak, J., Rockmann, T., and Brenninkmeijer, C. A. M.: Continuous-flow isotope analysis of the deuterium/hydrogen ratio in atmospheric hydrogen, Rapid Commun. Mass. Sp., 18, 299–306, doi:10.1002/rcm.1309, 2004.

Rice, A. L., Gotoh, A. A., Ajie, H. O., and Tyler, S. C.: High-

precision continuous-flow measurement of δ^{13}C and δD of atmospheric CH_4, Anal. Chem., 73, 4104–4110, 2001.

Rockmann, T., Jöckel, P., Gros, V., Bräunlich, M., Possnert, G., and Brenninkmeijer, C. A. M.: Using ^{14}C, ^{13}C, ^{18}O and ^{17}O isotopic variations to provide insights into the high northern latitude surface CO inventory, Atmos. Chem. Phys., 2, 147–159, doi:10.5194/acp-2-147-2002, 2002.

Rockmann, T., Kaiser, J., Brenninkmeijer, C. A. M., and Brand, W. A.: Gas chromatography/isotope-ratio mass spectrometry method for high-precision position-dependent ^{15}N and ^{18}O measurements of atmospheric nitrous oxide, Rapid Commun. Mass. Sp., 17, 1897–1908, doi:10.1002/rcm.1132, 2003.

Rudolph, J., Lowe, D. C., Martin, R. J., and Clarkson, T. S.: A novel method for compound specific determination of δ^{13}C in volatile organic compounds at ppt levels in ambient air, Geophys. Res. Lett., 24, 659–662, 1997.

Santrock, J., Studley, S. A., and Hayes, J. M.: Isotopic Analyses Based on the Mass Spectrum of Carbon Dioxide, Anal. Chem., 57, 1444–1448, 1985.

Schütze, M.: Ein neues Oxidationsmittel für die quantitative Uberführung von Kohlenmonoxyd in Kohlendioxyd, Ein Beitrag zur Chemie des Jodpentoxids, Ber. Dtsch. Chem. Ges, 77b, 484–487, 1949.

Schwander, J. and Stauffer, B.: Age Difference between Polar Ice and the Air Trapped in Its Bubbles, Nature, 311, 45–47, 1984.

Seiler, W.: Cycle of atmospheric CO, Tellus, 26, 116–135, 1974.

Smiley, W. G.: Note on a reagent for oxidation of carbon monoxide, Nucl. Sci. Abstr, 3, p. 391, 1949.

Stevens, C. M. and Krout, L.: Method of the determination of the carbon and of the oxygen isotopic composition of atmospheric carbon monoxide, Int. J. Mass Spectrom., 8, 265–275, 1972.

Stevens, C. M., Walling, D., Venters, A., Ross, L. E., Engelkem, A., and Krout, L.: Isotopic Composition of Atmospheric Carbon-Monoxide, Earth Planet. Sc. Lett., 16, 147–165, 1972.

Stevens, C. M. and Wagner, A. F.: The Role of Isotope Fractionation Effects in Atmospheric Chemistry, Z. Naturforsch. A, 44, 376–384, 1989.

Thompson, A. M.: The oxidizing capacity of the earth's atmosphere: probable past and future changes, Science, 256, 1157–1165, 1992.

Thompson, L. G., Mosley-Thompson, E., Davis, M. E., Lin, P. N., Henderson, K., and Mashiotta, T. A.: Tropical glacier and ice core evidence of climate change on annual to millennial time scales, Climatic Change, 59, 137–155, 2003.

Tsunogai, U., Nakagawa, F., Komatsu, D. D., and Gamo, T.: Stable Carbon and Oxygen Isotopic Analysis of Atmospheric Carbon Monoxide Using Continuous -Flow Isotope Ratio MS by Isotope Ratio Monitoring of CO, Anal. Chem., 74, 5659–5700, 2002.

Verschuren, D., Laird, K. R., and Cumming, B. F.: Rainfall and drought in equatorial east Africa during the past 1,100 years, Nature, 403, 410–414, 2000.

Wang, Z. H.: Records of Concentration, ^{13}C and ^{18}O of Atmospheric CO in the past, Ph.D. thesis, Stony Brook University, USA, 2009.